

Draft to be submitted to Nonlinearity

EXAMPLE OF SIMPLEST BIFURCATION DIAGRAM FOR A MONOTONE FAMILY OF VECTOR FIELDS ON A TORUS

CLAUDE BAESENS, MARC HOMES-DONES AND ROBERT S. MACKAY

Mathematics Institute, University of Warwick, UK.

ABSTRACT. We show that the bifurcation diagram proposed in Baensens *et al* (2018 *Nonlinearity* **31** 2928-2981) is the simplest bifurcation diagram for a monotone two-parameter family of vector fields on a torus. We achieve this by finding an example that satisfies all the minimal conditions derived there. We give proofs for all but one of the conditions and present strong numerical evidence for the remaining one.

1. INTRODUCTION

It was recently proven in [BM18] that any monotone family of vector fields on a torus has to have a global bifurcation diagram at least as complicated as the one proposed in the paper. Here we present a modification of the example in [BM18] that we believe does satisfy all the conditions of [BM18] and therefore has the simplest bifurcation diagram. We prove all but one of the conditions and give strong numerical evidence for the remaining one.

The setting is two-parameter families of vector fields

$$\dot{\mathbf{x}} = G(\mathbf{x}, \boldsymbol{\Omega})$$

with $\mathbf{x} \in \mathbb{T}^2 = \mathbb{R}^2/\mathbb{Z}^2$ and $\boldsymbol{\Omega} \in \mathbb{R}^2$ and $G \in \mathcal{C}^3$. We assume them to have monotone dependence on $\boldsymbol{\Omega}$ in the sense that for a given inner product $\langle \cdot, \cdot \rangle$ and $c > 0$,

$$\langle D_{\boldsymbol{\Omega}} G(\mathbf{x}, \boldsymbol{\Omega}) \mathbf{w}, \mathbf{w} \rangle \geq c|\mathbf{w}|^2$$

for all $(\mathbf{x}, \boldsymbol{\Omega}) \in \mathbb{T}^2 \times \mathbb{R}^2$ and $\mathbf{w} \in \mathbb{R}^2$, where $D_{\boldsymbol{\Omega}} G(\bar{\mathbf{x}}, \bar{\boldsymbol{\Omega}})$ is the derivative with respect to the second coordinate at $(\bar{\mathbf{x}}, \bar{\boldsymbol{\Omega}})$. We also want our family to be generic, in the sense that we consider a countable intersection of open dense subsets of \mathcal{C}^3 families, chosen to restrict the main bifurcations to have codimension at most two and the families to be transverse to them.

Under these conditions and by minimizing the sequence of features presented in [BM18], the proposed simplest bifurcation diagram satisfies the following assumptions:

1. there are at most two equilibria for any parameter values;

E-mail address: marc.homes-dones@warwick.ac.uk.

Date: July 11, 2022.

2020 Mathematics Subject Classification. 37E35, 37Gxx, 34C23 .

Key words and phrases. bifurcation, vector field, torus, simplest.

M. H.-D. was supported by “la Caixa” Foundation (ID 100010434) with fellowship code LCF/BQ/EU20/11810061.

- 2.** there are at most four B points (parameter with Bogdanov-Takens bifurcation);
- 3a.** there is no closed curve of centre nor closed curve of neutral saddle;
- 3b.** there is no coexistence of centre and neutral saddle;
- 4a.** there are at most two Reeb components for parameter values in the hole;
- 4b.** there is no other invariant annulus for flows in the hole;
- 4c.** there is no Reeb component for parameters outside the resonance region;
- 5a.** there are at most four Z points on the inner saddle-node curve;
- 5b.** there are at most four Z points of horizontal homotopy types on the outer saddle-node curve;
- 5c.** there are at most four curves of rotational homoclinic connection (rhc) of horizontal homotopy types;
- 6.** there are at most two necklace (N) points;
- 7a.** there is no contractible homoclinic connection to a neutral saddle (J point);
- 7b.** there is at most one contractible periodic orbit for any parameters;
- 8.** there are at most four K points for horizontal homotopy types;
- 9.** there are at most two H points.

We will introduce most of the notation used above throughout the text, but one can find an index of all¹ the terms in the introduction of [BM18].

We present strong evidence that the family of vector fields,

$$\begin{aligned}\dot{x} &= \Omega_x - \cos 2\pi(y - \phi) - \varepsilon \cos 2\pi x \\ \dot{y} &= \Omega_y - \sin 2\pi y - \varepsilon \sin 2\pi x\end{aligned}\tag{\#}$$

where ε is small and positive and $\phi \in (\frac{1}{24}, \frac{5}{24})$ satisfies all the above assumptions. For future reference note that

$$\cos 2\pi(y - \phi) = C \cos 2\pi y + S \sin 2\pi y,$$

where $C = \cos 2\pi\phi > 0$, $S = \sin 2\pi\phi > 0$.

In [BM18], the case $\phi = 0$ was considered, but it was found that there were four degenerate Hopf bifurcations which caused the appearance of more than one *contractible periodic orbit* (cpo) in some regions of parameter space, thus contradicting assumption 7b. This motivated our introduction of ϕ , which enables us to tune the system, and as we will see in appendix C, eliminates the degenerate Hopf points when $\phi \in (\frac{1}{24}, \frac{5}{24})$. Another apparent obstruction to satisfy assumption 7b, was that in [BM18] it was erroneously computed that the necklace points were outside the trace-zero loops. This error was corrected in the corrigendum [BLM22] together with numerical computation of the relevant part of the bifurcation diagram.

We give proofs that all the assumptions are satisfied for the modified example (#), except for assumption 7b which we were only able to validate numerically, see section 4. To get a formal proof an insight is needed to determine the sign of the integrals (4.1) which would automatically give at most one cpo.

This paper should be read as a companion paper to [BM18]. We will often refer to it for the methodology of the proofs and its figures. When appropriate though, we have fleshed out arguments that were only sketched there, for instance see the study of snp curves in section 5.1.

¹Except for Z point, which is a parameter value where the saddle-node has a rhc between the neutral direction and the hyperbolic one.

2. FIRST PROPERTIES

Besides the assumptions listed in the introduction, we also need to check that our family is \mathcal{C}^3 and monotone, both of which are immediate for our example (considering standard inner product). Moreover, for the principal features of the bifurcation diagram (saddle-node equilibria, Hopf bifurcation, Bogdanov–Takens points, and horizontal homoclinic connections), we will check throughout the text that they are codimension at most two with our family being transverse to them. It is probably unfeasible to check this for all features, as there are infinitely many partial mode-locking tongues, but appealing to \mathcal{C}^3 -genericity we can deduce that there are arbitrary small \mathcal{C}^3 perturbations of our example satisfying this.

2.1. Equilibria. The equilibria of (#) are given by,

$$\begin{aligned}\Omega_x &= \cos 2\pi(y - \phi) + \varepsilon \cos 2\pi x \\ \Omega_y &= \sin 2\pi y + \varepsilon \sin 2\pi x.\end{aligned}\tag{2.1}$$

The set E of equilibria (Ω, \mathbf{x}) as a subset of $\mathbb{R}^2 \times \mathbb{T}^2$ is the graph of the function $\Omega^\varepsilon : \mathbb{T}^2 \rightarrow \mathbb{R}^2$ defined by (2.1). Furthermore, when y and x rotate around the torus, $\Omega^\varepsilon(\mathbf{x})$ performs similar movement to an epicycle, where the base circle is replaced by the ellipse²

$$\psi(y) = (\cos 2\pi(y - \phi), \sin 2\pi y)\tag{2.2}$$

and the other is a circle of radius ε . We define the resonance region R as the projection of E onto \mathbb{R}^2 or equivalently the image of Ω^ε . So by the description with epicycles, R is a closed ε -neighbourhood of the ellipse ψ , see [BM18, Figure 23(a)] for the case $\phi = 0$ when ψ is a circle.

2.1.1. Parametrisation of the resonance region. For ε small enough we can parametrise the ε -neighbourhood of ψ by its tubular neighbourhood, i.e. R can be parametrised by,

$$\Omega = \gamma_r(\theta) := \psi(\theta) + rN_\psi(\theta),\tag{2.3}$$

where N_ψ is the external unit normal vector of ψ , $\theta \in \mathbb{T}^1$ and $|r| \leq \varepsilon$. So in this case, the boundary of R is given by

$$\gamma_\pm(\theta) := \gamma_{\pm\varepsilon}(\theta) = \psi(\theta) \pm \varepsilon N_\psi(\theta).\tag{2.4}$$

By studying for which r the curve γ_r stops being regular one finds that (2.3) is injective, and thus gives a parametrisation, as long as $r > -\frac{1}{\kappa_{\max}}$ where κ_{\max} is the maximum curvature of ψ . So ε small enough in the start of this section can be quantified by $\varepsilon < \frac{1}{\kappa_{\max}}$. Moreover, for $r > \varepsilon$, equation (2.3) is also a parametrisation, that covers the unbounded component of the complement of R , which we will refer to as the “outside” of R .

²Note that when $\phi = \pm\frac{1}{4}$, the ellipse ψ degenerates to a line segment. This does not happen in our context as $\phi \in (\frac{1}{24}, \frac{5}{24})$.

2.1.2. *Checking assumption 1.* We check that when $\varepsilon < \frac{1}{\kappa_{\max}}$, there are precisely two equilibria for each interior point of R and one for each boundary point of R , so that assumption 1 is satisfied.

For a fixed y and varying $x \in \mathbb{T}^1$, $\Omega^\varepsilon(\mathbf{x})$ makes a circle centred at $\psi(y)$ of radius ε , which by (2.4) intersects the inner (resp. outer) boundary of R at precisely one point, see green dashed circle in [BM18, Figure 23(a)]. Then, doing a positive lap of y moves this circle and the intersections anticlockwise making a full lap around the “hole”, i.e. the bounded component of the complement of R . Thus, each of the two arcs of the circle with end points in ∂R go through every point $\Omega \in R$ precisely once. Hence, we have exactly two equilibria for parameters in the interior of R and only one in the boundary as both arcs coincide there.

2.2. **Linearisation at equilibria.** Given parameters Ω let us linearise the vector-field around an equilibrium (x, y) , for tangent orbit $(\delta x, \delta y)$,

$$\begin{pmatrix} \dot{\delta x} \\ \dot{\delta y} \end{pmatrix} = \begin{pmatrix} 2\pi\varepsilon \sin 2\pi x & 2\pi \sin 2\pi(y - \phi) \\ -2\pi\varepsilon \cos 2\pi x & -2\pi \cos 2\pi y \end{pmatrix} \begin{pmatrix} \delta x \\ \delta y \end{pmatrix}. \quad (2.5)$$

The matrix determinant is,

$$\det = 2\pi\varepsilon(\cos 2\pi x, \sin 2\pi x) \cdot \psi'(y),$$

where ψ was defined in (2.2), so $\det = 0$ when $(\cos 2\pi x, \sin 2\pi x) \perp \psi'(y)$, or equivalently when $(\cos 2\pi x, \sin 2\pi x) = \pm N_\psi(y)$. By (2.4), this happens precisely when Ω is in the boundary of R . So in the boundary of R we have saddle-nodes if $\text{tr} \neq 0$ which are generic as shown in appendix A. We also see that \det is positive in the interior of one of the two copies of R that form E , where the equilibrium has Poincaré index $+1$ and \det is negative in the other copy of R , where the equilibrium has index -1 , see [BM18, Figure 24(a)].

The linearised vector field has trace,

$$\text{tr} = 2\pi(\varepsilon \sin 2\pi x - \cos 2\pi y).$$

Thus the trace is zero where $\cos 2\pi y = \varepsilon \sin 2\pi x$, which form two closed curves on E , one near $y = \frac{1}{4}$ and the other one near $y = -\frac{1}{4}$. The trace of both equilibria is negative on the part projecting to the right of these curves, and positive to the left, whereas in the region enclosed by the projection of these curves (we will show they are simple curves in section 2.2.2) the sign differs between equilibria, see [BM18, Figure 24(b)].

2.2.1. *B points.* We study when both tr and \det vanish. Let $x(y)$ be implicitly defined by one of the curves $\det = 0$ and recall that tr can only vanish at $y = \pm\frac{1}{4} + O(\varepsilon)$, where

$$\frac{d}{dy} \text{tr}(x(y), y)|_{y=\pm\frac{1}{4}+O(\varepsilon)} = \pm 4\pi^2 + O(\varepsilon).$$

So we have a single simple zero close to $y = \frac{1}{4}$ and another one close to $y = -\frac{1}{4}$ for each $\det = 0$ curve. These 4 points have double eigenvalue zero, with non-diagonal Jordan form as the entries of (2.5) can not all simultaneously vanish. Thus, they are B points and assumption 2 is satisfied. We check that they are generic B points in appendix B.

2.2.2. *Trace-zero curves.* The part of each trace-zero curve with index +1 consists of centers, and the trace has non-zero derivative across it, so these are curves of Hopf bifurcations. Crucially, we show in appendix C, that they are generic Hopf bifurcations, in contrast to the system with $\phi = 0$, studied in [BM18], which had four points of degenerate Hopf bifurcation. Thus, our example avoids the obstruction to having at most one cpo and so there is hope of satisfying assumption 7b.

The part of each trace-zero curve with index -1 consists of *neutral saddle* (ns), where the eigenvalues are equal in magnitude but opposite in sign. The derivative of the trace across it is non-zero too, which will be needed later. So each curve of trace-zero consists of an arc of center and an arc of ns. As there are no closed curves of center nor closed curves of ns, assumption 3a is satisfied.

We now study the projection of the trace-zero curves to R . We know they are near $y = \pm\frac{1}{4}$, so they are within $O(\varepsilon)$ of $\Omega_x = \pm S$, $\Omega_y = \pm 1$. We also have shown that each curve touches each boundary of R once, in the B points. Using that $\varepsilon \sin 2\pi x = \cos 2\pi y$ together with (2.1), we find that the trace-zero curves are parametrised to first order by

$$\begin{aligned}\Omega_x &= \pm S + \varepsilon(\cos 2\pi x + C \sin 2\pi x) + O(\varepsilon^2) \\ \Omega_y &= \pm 1 + \varepsilon \sin 2\pi x + O(\varepsilon^2),\end{aligned}$$

where the differential with respect to x of the error terms is also $O(\varepsilon^2)$. So we deduce that the trace-zero curves are mapped to simple closed curves in the parameter space \mathcal{C}^1 -close to the ellipses,

$$(\Omega_x - C\Omega_y \pm (C - S))^2 + (\Omega_y \mp 1)^2 = \varepsilon^2. \quad (2.6)$$

In particular there is no simultaneous center and ns, proving assumption 3b.

2.3. **Flow outside the resonance region.** Outside of R , we show there is Poincaré flow, i.e. the flow has a cross-section. By the arguments in [BM18] to check the existence of a cross-section, it is enough to find a linear combination f of x and y , such that $\dot{f} > 0$.

Let Ω be outside the resonance region, then by the comments made in section 2.1.1, we have $\Omega = \psi(\theta) + rN_\psi(\theta)$, for some angle θ and $r > \varepsilon$. Then, define

$$f = \langle N_\psi(\theta), (x, y) \rangle$$

(on the universal cover \mathbb{R}^2 of \mathbb{T}^2), we have,

$$\dot{f} = \langle -N_\psi(\theta), \psi(y) - \psi(\theta) \rangle + (r - \varepsilon \langle N_\psi(\theta), (\cos 2\pi x, \sin 2\pi x) \rangle).$$

The second term is positive as $r > \varepsilon$ and the scalar product of two unit vectors is bounded by one. The first term is non-negative as the angle of the internal normal of an ellipse at a point with a chord containing that point is acute. Thus, $\dot{f} > 0$.

2.4. **Flow in $|\Omega_y| < 1 - \delta$.** Next, we examine the flow for parameters in a strip $|\Omega_y| < 1 - \delta$ with $\delta = K\varepsilon$ for a large enough K (chosen independently of ε).

This study follows exactly in the same way as the case $\phi = 0$ presented in [BM18]. We even get quantitatively the same results in the crucial degenerate case $\varepsilon = 0$, except for having an ellipse instead of a circle as resonance region and having the horizontal velocity in the invariant circles given by

$$\dot{x} = \Omega_x \mp C\sqrt{1 - \Omega_y^2} - S\Omega_y.$$

So as in [BM18], in this regions of parameters we have exactly two \mathcal{C}^1 invariant circles of horizontal homotopy type, which contain the ω and α limit sets of any point. In the hole, these invariant circles are periodic orbits with opposite directions, thus bounding two *Reeb components*. Outside R they are periodic orbits with the same direction, thus forming a Poincare flow, see [BM18, Figure 25].

Now if in $\Omega_x \geq 0$ we move our parameters from the hole to the outside of R , we see that the attracting periodic orbit experiences a *saddle-node on an invariant circle* (snic) bifurcation on entering the resonance regions, then the equilibria do roughly half a revolution in opposite directions meeting and experiencing another snic bifurcation when leaving the resonance region, see figure [BM18, Figure 25]. We have the same behaviour for the repelling circle in $\Omega_x \leq 0$.

2.5. Flow in $|\Omega_y \mp 1| \leq \delta$ and $|\Omega_x \mp S| \leq \sqrt{3\delta}$. We now consider all parameters not studied in the previous sections that are close to the resonance region. Thus, we are interested in finding where the resonance region intersects the bands $|\Omega_y \mp 1| \leq \delta$. Using that the resonance region is a ε -neighbourhood of the ellipse ψ we find that

$$|\Omega_x \mp S| \leq C\sqrt{\delta(2 + 1/K)} + O(\delta),$$

so for δ small and $K > 1$ we certainly have $|\Omega_x \mp S| \leq \sqrt{3\delta}$. The factor 3 is missing in [BM18] due to a computational error. Without loss of generality, from now on we will study the top of the resonance region, i.e. $|\Omega_y - 1| \leq \delta$ and $|\Omega_x - S| \leq \sqrt{3\delta}$.

Inspired by (2.3) we consider the parametrization,

$$\Omega = \psi(\theta) + \varepsilon\rho N_\psi(\theta), \quad (2.7)$$

so the resonance region is $|\rho| \leq 1$. If we let $\theta = \frac{1}{4} - \sqrt{\varepsilon}\alpha$ one finds Taylor expanding (2.7) that the region of parameters studied in this section has $\rho, \alpha = O(1)$. Now as $\Omega_y = 1 + O(\varepsilon)$, outside a neighbourhood of order $\sqrt{\varepsilon}$ of $y = \frac{1}{4}$, $\dot{y} > 0$, and the flow eventually reaches this neighbourhood. Thus it is enough to study the flow in the regime $y = \frac{1}{4} + O(\sqrt{\varepsilon})$ which we do by letting,

$$y = \frac{1}{4} + \sqrt{\varepsilon}\eta$$

and as in this region the motion is slow we take $s = \sqrt{\varepsilon}t$ and use $'$ for $\frac{d}{ds}$. Then, Taylor expanding (#) in these coordinates we get,

$$\begin{aligned} x' &= 2\pi C(\eta + \alpha) + O(\sqrt{\varepsilon}) \\ \eta' &= 2\pi^2(\eta^2 - \alpha^2) + \rho - \sin 2\pi x + O(\varepsilon). \end{aligned} \quad (2.8)$$

This is precisely the first order approximation found for the case $\phi = 0$ in [BM18], except that in that case $C = 1$. This does not change the analysis at all, so the same arguments hold and we get the following conclusions.

For parameter values in the hole, the vector field consist of precisely two Reeb components, thus our example satisfies assumption 4a and 4b.

In the top of the resonance region there are precisely two curves where the vector field has a generic horizontal *rotational³ homoclinic connection* (rhc). Moreover, these curves are given by smooth graphs $\alpha^\pm(\rho)$. There are no other horizontal rhc curves, besides the analogous ones in the bottom of R so assumption 5c is satisfied. The two rhc curves from the top of the resonance intersect at $\alpha = O(\sqrt{\varepsilon})$ forming

³We will use *rotational* as a short hand for ‘‘homotopically non-trivial’’.

an N point, see [BM18, Figure 34]. Uniqueness of this intersection will be deduced in section 3.2.

Each rhc curve meets each boundary curve of R once where we have a Z point, see [BM18, Figure 8]. So we have precisely four Z points of horizontal homotopy type in each curve of the resonance's boundary, thus justifying assumptions 5a. It also justifies assumption 5b, as in the inner boundary we have horizontal homological direction.

Assuming genericity, we can deduce that in the band $|\rho - 2\pi^2\alpha^2| < 1$ and to the right (resp. left) of a δ -neighbourhood of $\Omega = (S, 1)$, we have a curve of horizontal *saddle-node periodic orbits* (snp) above the corresponding rhc curve, see [BM18, Figure 31]. The snp could possibly have cusps and self-intersections, though they would imply regions with more than two horizontal periodic orbits. We did not rule this out but consider it unlikely; moreover it does not directly affect any of the properties we want our system to satisfy.

To finish this section we argue that outside a δ -neighbourhood of $\Omega = (S, 1)$ there is no *contractible homoclinic connection* (chc) nor *contractible periodic orbit* (cpo). We give a detailed explanation here as this was not explicitly shown in [BM18]. First note that the trace of (2.8) is,

$$\text{tr} = 4\pi^2\eta + O(\sqrt{\varepsilon}), \quad (2.9)$$

and as the possible equilibria are located at $\eta = -\alpha + O(\sqrt{\varepsilon})$ they have $\text{tr} = -4\pi^2\alpha + O(\sqrt{\varepsilon})$. Now, using (2.9) and the first equation in (2.8), we find that a cpo γ with period T would have Lyapunov exponent

$$\frac{1}{T} \int_{\gamma} \text{tr} ds = \frac{4\pi^2}{T} \int_{\gamma} \frac{x'}{2\pi C} - \alpha ds + O(\sqrt{\varepsilon}) = -4\pi^2\alpha + O(\sqrt{\varepsilon})$$

where in the last equality we have used that γ is contractible so $\int_{\gamma} x' ds = 0$. Thus, the sign of the Lyapunov exponent coincides with the sign of the trace at the equilibria if α is not small. This regime corresponds to parameters outside a δ -neighbourhood of $(S, 1)$ if K in δ is big enough. We can conclude that there cannot exist cpos in this regime, as they would have the same attracting/repelling nature as the node and would give rise to impossible phase portraits. Essentially the same argument shows that there are no chc either.

3. δ -NEIGHBOURHOOD OF TOP AND BOTTOM OF RESONANCE REGION

To complete our analysis of the vector field, we zoom in on a δ -neighbourhood of $\Omega = (1, S)$ (similar analysis could be done for $\Omega = (-1, -S)$). Here, we derive an approximation for the vector field which is reversible (conjugate to its time-reverse). We use the remainder terms to prove that for small ε there is a unique N point, precisely two K points, a unique H point, and the N point is connected to the B points by arcs of chc.

3.1. Reversible approximation. To study a δ -neighbourhood of $\Omega = (1, S)$ we specialize the approximation in (2.8) by letting $\alpha = \sqrt{\varepsilon}\tilde{\alpha}/2\pi$, while also including the order $\sqrt{\varepsilon}$ terms in the Taylor expansion, so

$$\begin{aligned} x' &= 2\pi C\eta + \sqrt{\varepsilon}(C\tilde{\alpha} - \cos 2\pi x + 2\pi^2 S\eta^2) + O(\varepsilon) \\ \eta' &= \rho - \sin 2\pi x + 2\pi^2\eta^2 + O(\varepsilon) \end{aligned}$$

In this section we study the unperturbed case $\varepsilon = 0$,

$$\begin{aligned} x' &= 2\pi C\eta \\ \eta' &= \rho - \sin 2\pi x + 2\pi^2\eta^2 \end{aligned} \quad (3.1)$$

which is a family of reversible vector fields with respect to the reflection $\eta \rightarrow -\eta$, with one parameter ρ . This family coincides with the approximation found in [BM18], except that there $C = 1$. Hence, by the same arguments we find that in the universal cover it is Hamiltonian with respect to the symplectic form,

$$\mathcal{A} = e^{-2\pi x} dx \wedge d\eta.$$

That is, the system $e^{-2\pi x/C} x'$ and $e^{-2\pi x/C} \eta'$ has Hamiltonian,

$$H(x, \eta) = e^{-2\pi x/C} \left(C\pi\eta^2 + \frac{C\rho}{2\pi} - \frac{1}{4\pi}g(x) \right)$$

where

$$g(x) = \frac{2C}{C^2 + 1} (C \cos 2\pi x + \sin 2\pi x)$$

which is found by solving the relation $\frac{1}{2C}g(x) - \frac{1}{4\pi}g'(x) = \sin 2\pi x$. This can be rewritten as,

$$g(x) = \frac{2C}{\sqrt{C^2 + 1}} \cos 2\pi(x - x_g)$$

with $x_g = \frac{1}{2\pi} \arctan C^{-1}$, where we can take the standard determination of arctangent from $-\frac{\pi}{2}$ to $\frac{\pi}{2}$ as $C > 0$.

The equilibrium points of the system are at $\eta = 0$ and $\sin 2\pi x = \rho$, the saddle is at $x_{\text{sad}} \in (\frac{1}{4}, \frac{3}{4})$ and the center at $x_{\text{cen}} \in (-\frac{1}{4}, \frac{1}{4})$. At the parameter value $\rho_0 = -1/\sqrt{1 + C^2}$, the system has a necklace point, with homoclinic loops given by

$$\eta = \pm \frac{(1 + C^2)^{-1/4}}{\pi} \cos \pi(x - x_g). \quad (3.2)$$

For $\rho \in (-1, \rho_0)$ the level set includes a contractible homoclinic loop to the right of the saddle whereas for $\rho \in (\rho_0, 1)$ it has a contractible homoclinic loop to the left. Each contractible homoclinic loop bounds a region foliated by cpos around the centre, see [BM18, Figure 33].

In the following sections we use Pontryagin's energy balance method to determine where various features of the reversible approximation persist on adding the correction terms.

3.2. Rotational homoclinic connection (rhc) and necklace point (N). First, we compute where the unperturbed rhc^\pm given by (3.2) persist by letting $\rho = \rho_0 + \sqrt{\varepsilon}\tilde{\rho}$. If we denote by γ_\pm the unperturbed rhc^\pm from $x_g - 1/2$ to $x_g + 1/2$, using Pontryagin's method as in [BM18], we see that they persist when

$$\Delta H = \int_{\gamma_\pm} \dot{H} dt + O(\varepsilon) = \sqrt{\varepsilon}(c\tilde{\rho} \mp Ca\tilde{\alpha} + b) + O(\varepsilon) = 0,$$

where,

$$\begin{aligned} a &= \frac{-1}{\sqrt[4]{1+C^2}} \int_{\gamma_+} e^{-2\pi x/C} \sin \pi(x-x_g) dx = k\sqrt{1+C^2}, \\ b &= \frac{-1}{\sqrt[4]{1+C^2}} \int_{\gamma_+} e^{-2\pi x/C} \sin \pi(x-x_g) \left(\cos 2\pi x - \frac{2S \cos^2 \pi(x-x_g)}{\sqrt{1+C^2}} \right) dx \\ &= -k \frac{2C^2(C+2S)}{4+9C^2}, \\ c &= \int_{\gamma_+} e^{-2\pi x/C} dx = \frac{k}{4} (1+C^2)^{3/4} (4+C^2) \tanh \frac{\pi}{C}, \end{aligned}$$

with

$$k = \frac{4C e^{-C^{-1} \arctan C^{-1}} \cosh \frac{\pi}{C}}{\pi (1+C^2)^{3/4} (4+C^2)}.$$

Thus, to leading order

$$\tilde{\rho} = \pm (Ca\tilde{\alpha} - b)/c,$$

and the approximate curves rhc^\pm cross transversely at $\tilde{\rho} = 0$ and

$$\tilde{\alpha} = \frac{b}{Ca} = -\frac{2C(C+2S)}{(4+9C^2)\sqrt{1+C^2}} \quad (3.3)$$

forming an N point.

There is no other horizontal rhc in $|\rho| \leq 1$, $\tilde{\alpha} = O(1)$, because the phase portraits for the reversible approximation allow such feature only near $\rho = \rho_0$, where the Pontryagin's method above gives the locally unique curves found. So the N point found above is unique in this region of parameters, which by section 2.5, is the only possible location of an N point in the top of the resonance. Doing the same for the bottom we prove assumption 6.

To determine the local behaviour around the N point we need the sign of the trace at the saddle. From (2.6) we deduce that the zero-trace loop in $(\tilde{\alpha}, \rho)$ parameters is \mathcal{C}^1 -close to the ellipse

$$\rho^2 + C^2(\tilde{\alpha} - \rho)^2 = 1. \quad (3.4)$$

Thus substituting (3.3) and ρ_0 we see that the N point is inside the trace-zero loop. In particular it is to the right of the ns curve, so the trace in the saddle is negative which produces the unfolding depicted in [BM18, Figure 34]. Note that, as mentioned in the corrigendum [BLM22], in the case $\phi = 0$ we also get the N point inside the trace-zero loop.

3.3. Contractible homoclinic connection (chc). Next we compute how the contractible homoclinic connections of the reversible approximation persist for each $\rho \in (-1, \rho_0) \cup (\rho_0, 1)$. Following [BM18], we see that there are unique curves of chc close to $\tilde{\alpha}(\rho) = b(\rho)/Ca(\rho)$, where

$$\begin{aligned} a(\rho) &= \int_{\gamma} e^{-2\pi x/C} d\eta = \frac{2\pi}{C} \int_{\bar{\gamma}} e^{-2\pi x/C} dx d\eta > 0, \\ b(\rho) &= \int_{\gamma} e^{-2\pi x/C} (\cos 2\pi x - 2\pi S \eta^2) d\eta = \frac{2\pi}{C} \int_{\bar{\gamma}} e^{-2\pi x/C} (f(x) + S\rho) dx d\eta, \end{aligned} \quad (3.5)$$

with γ the unperturbed chc , $\bar{\gamma}$ the region bounded by it, and

$$f(x) = \cos 2\pi x + (C - S) \sin 2\pi x.$$

The chc tends to the concatenation of the two rhcs as $\rho \rightarrow \rho_0$ thus $b(\rho)/Ca(\rho) \rightarrow b/Ca$ from (3.3), i.e. the chc curves tend to the necklace as $\rho \rightarrow \rho_0$, which is consistent with the unfolding of the N point [BM18, Figure 34].

Note that $\tilde{\alpha} = b(\rho)/Ca(\rho)$, can be interpreted as the average value of $(f+S\rho)/C$, in the region $\bar{\gamma}$, weighted by $e^{-2\pi x/C}$. As when $\rho \rightarrow \pm 1$ the chc shrinks to a point then $\tilde{\alpha}$ tends to the value of $(f+S\rho)/C$ in the center. Thus, using $\sin 2\pi x_{\text{cen}} = \rho$, we find $\tilde{\alpha} \rightarrow \pm 1$ when $\rho \rightarrow \pm 1$. These are the locations of the B points, which can be deduced from (3.4) and the fact that in the boundary of the resonance $\rho = \pm 1$. In conclusion, the chc curves connect the B points to the N point.

Finally, we prove that the curves of chc do not intersect that of ns, so there is no J point, justifying assumption 7a. Using $\sin 2\pi x_{\text{sad}} = \rho$ and (3.4), we find that the curve of ns has

$$\tilde{\alpha} \sim (C \sin 2\pi x_{\text{sad}} + \cos 2\pi x_{\text{sad}})/C.$$

Thus, proving $\tilde{\alpha}_{\text{chc}} > \tilde{\alpha}_{\text{ns}}$ is equivalent to showing that the average of f over the region bounded by chc (weighted by $e^{2\pi x/C}$) is bigger than $f(x_{\text{sad}})$. Showing this is tedious and not particularly insightful when $\phi \neq 0$, see appendix D.

4. CONTRACTIBLE PERIODIC ORBITS

In this section we show numerically that the cpos of the reversible approximation give rise to a unique cpo for each parameter value in the zone between the curve of chc and the curve of centres, see [BM18, Figure 15]. Our analysis also shows that no cpo persist for parameters outside this region. Moreover, the phase diagram of the reversible approximation does not allow for the appearance of any other cpo. As we showed in section 2.4 and 2.5 that there are not cpos for parameters outside a δ -neighbourhood of the top and bottom of the resonance region, we can conclude that assumption 7b is satisfied.

Using Pontryagin's method exactly as in section 3.3, we find that a cpo γ with energy E persists only along $\tilde{\alpha}(E, \rho) = b(E, \rho)/Ca(E, \rho)$, where a, b are given by (3.5), or equivalently,

$$a(E, \rho) = \frac{4\pi}{C} \int_{x_{\min}}^{x_{\max}} e^{-2\pi x/C} \eta dx,$$

$$b(E, \rho) = \frac{4\pi}{C} \int_{x_{\min}}^{x_{\max}} (f + S\rho) e^{-2\pi x/C} \eta dx,$$

with x_{\min}, x_{\max} the intersections of γ with the x -axes, and $\eta \geq 0$ in γ . If we denote by $E_{\text{cen}}, E_{\text{sad}}$ the energy at the center and saddle respectively we have $E_{\text{cen}} \leq E_{\text{sad}}$ and $E \in (E_{\text{cen}}, E_{\text{sad}})$. When $E \rightarrow E_{\text{sad}}$, the cpo tends to the chc, so we get $\tilde{\alpha}(E, \rho) \rightarrow \tilde{\alpha}(\rho)$ from section 3.3. Note that, as in the case of chc, $\tilde{\alpha}(E, \rho)$ can be interpreted as the average of the function $(f+S\rho)/C$ (weighted by $e^{-2\pi x/C}$) in the region bounded by the cpo. So when $E \rightarrow E_{\text{cen}}$ and the cpo shrinks to a point, $\tilde{\alpha}(E, \rho)$ tends to the value of the function at the centre. Using that $\sin 2\pi x_{\text{cen}} = \rho$ we find that as $E \rightarrow E_{\text{cen}}$,

$$\tilde{\alpha}(E, \rho) \rightarrow C\rho + \sqrt{1 - \rho^2},$$

which from (3.4), is the value of $\tilde{\alpha}$ at the centre.

Now if we show that for a fixed $\rho \in (-1, 1)$, $\tilde{\alpha}(E, \rho)$ is strictly decreasing in the interval $(E_{\text{cen}}, E_{\text{sad}})$, then we can conclude that for each parameter in the region between the chc curve, and the centre curve, we have exactly one cpo.

To show that $\tilde{\alpha}(E, \rho)$ is decreasing on E , we compute its derivative,

$$\tilde{\alpha}'(E, \rho) := \frac{\partial \tilde{\alpha}}{\partial E}(E, \rho) = \frac{a'b - ab'}{b^2} \quad (4.1)$$

where everything in the right is evaluated at (E, ρ) , and

$$a'(E, \rho) := \frac{\partial a}{\partial E}(E, \rho) = \frac{4\pi}{C} \int_{x_{\min}}^{x_{\max}} \frac{1}{C^2 \eta} dx,$$

$$b'(E, \rho) := \frac{\partial b}{\partial E}(E, \rho) = \frac{4\pi}{C} \int_{x_{\min}}^{x_{\max}} \frac{f}{C^2 \eta} dx,$$

which have been computed by differentiating under the integral sign, while using that $\eta(x_{\min}) = \eta(x_{\max}) = 0$.

As we are not able to compute the integrals, nor derive useful bounds on (4.1), we check the sign of $\tilde{\alpha}'$ numerically.

To present the numerical computations we chose $\phi = \frac{1}{8}$, which is enough to have an example of the simplest bifurcation diagram. We note though, that we have not seen significant difference with other values $\phi \in (\frac{1}{24}, \frac{5}{24})$. Figure 1 depicts a **Mathematica** density plot of $\tilde{\alpha}'$ in the region bounded by the center curve and the chc curves. As the density plot does not have blue regions, or even light yellows, we are fairly confident that the value of $\tilde{\alpha}'$ is always negative and significantly away from zero. We can conclude then that $\tilde{\alpha}$ is decreasing on E .

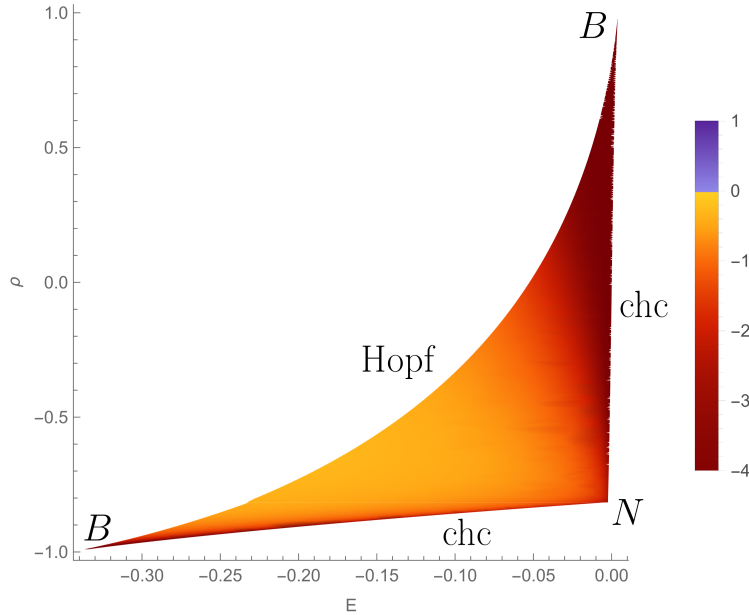


FIGURE 1. Density plot of $\tilde{\alpha}'$ in the regime of interest with $\phi = 1/8$. The region is bounded by two chc curves and a curve of centers where we have Hopf bifurcations.

To end this section we note that in the density plot it seems that $\tilde{\alpha}'$ has singularities at the B points, this is expected for generic B points.

5. K AND H POINTS

Finally, we find the intersections of rhc^\pm curves with the ns and the horizontal snp curves, which give K and H points respectively, see [BM18, Figure 16 and 20].

The same arguments as in [BM18] show that in the top of the resonance region each rhc^\pm curve intersects the curve of ns once, giving two K points of horizontal homotopy type. The only computational difference is that at the intersection the curve of ns has $d\tilde{\alpha}/d\rho \sim -S^2/C^2$, and that the K points are located near

$$\tilde{\alpha} = 2\rho_0, \quad \tilde{\rho} = \frac{-16C(2 - SC + 4C^2)}{(1 + C^2)^{3/4}(4 + C^2)(4 + 9C^2) \tanh \frac{\pi}{C}}.$$

Moreover, as these intersections are transverse and the trace has non-zero derivative across the ns curve, the K points are generic. Putting together the top and the bottom of the resonance region proves Assumptions 8.

Exactly as in [BM18] we find that the K point produces two curves of snp as depicted in [BM18, Figure 39]. Thus to conclude that there exists precisely one H point on the top of the resonance region it is enough to show that the snp^+ curve is \mathcal{C}^1 close to rhc^+ in the region of parameters $\tilde{\alpha}, \tilde{\rho}$. In a neighbourhood of the K point this follows from its generality, see [Per94]. It is not clear whether this neighbourhood covers all parameters of interest, so we do an explicit argument here for parameters outside this neighbourhood.

5.1. Transit map. The saddle is near $x_g + \frac{1}{2}$ so it is natural to consider the transit map \mathcal{T} from $x = x_g$ to $x = x_g + 1$. This map will be defined for $\eta > \eta_s$, the value of the stable manifold at x_g , and will be mapped to $\hat{\eta} > \eta_u$, the value of the unstable one at $x_g + 1$. We will use the coordinate $z = \eta^2$ as it will simplify some formulae.

Using the Hamiltonian with $\rho = \rho_0$ we find that in the unperturbed case the transit map is simply,

$$\mathcal{T}(z) = e^{2\pi/C}(z - K), \quad (5.1)$$

with $K = (e^{-2\pi/C} - 1)\rho_0/\pi^2 > 0$ and $z_s = z_u = -\rho_0/\pi^2 > 0$. In the perturbed case $z_u = z_s$ whenever there exists a rhc^+ . Recall that in section 3.2, we found that rhc^+ can be detected by the zeros of

$$\Delta H = H_u - H_s = \sqrt{\varepsilon}(c\tilde{\rho} - Ca\tilde{\alpha} + b) + O(\varepsilon),$$

where $H_{s/u}$ correspond to the energy at $(x_g, \eta_{s/u})$, as in section 3.2 we consider rhc between $x_g \pm \frac{1}{2}$. Converting to z using the Hamiltonian we find that,

$$z_u - z_s = K_1(H_u - H_s) \quad \text{with} \quad K_1 = e^{2\pi x_g/C}/(C\pi).$$

Thus the rhc^+ is defined by,

$$z_u - z_s = K_1\sqrt{\varepsilon}(c\tilde{\rho} - Ca\tilde{\alpha} + b) + O(\varepsilon) = 0, \quad (5.2)$$

where it is known that $z_u - z_s$ is differentiable respect parameters. Moreover the derivatives can be computed using the equation above as the differential of the error term keeps its order, i.e. it is $O(\varepsilon)$.

Going back (5.1) we note that the slope of the perturbed transit map is close to $e^{2\pi/C}$ away from the stable and unstable manifold, so no snp there. Thus, it is left to study $\mathcal{T}'(z)$ when z is close to z_s .

Consider now the evolution of the symplectic area $\mathcal{A} = e^{-2\pi x} dx \wedge d\eta$,

$$\dot{\mathcal{A}} = \mathcal{A}\tau, \quad \tau = 2\pi\sqrt{\varepsilon} \left(\sin 2\pi x - \tilde{\alpha} + \frac{1}{C} \cos 2\pi x - 2\pi^2 \frac{S}{C} \eta^2 \right) + O(\varepsilon). \quad (5.3)$$

So if we consider γ the path that the flow from (x_g, η) to $(x_g + 1, \hat{\eta})$ we have,

$$\frac{\hat{\mathcal{A}}}{\mathcal{A}} = e^{\int_{\gamma} \tau ds}. \quad (5.4)$$

An interpret of \mathcal{A} for the transit map is $e^{-2\pi x/C} 2\pi C \eta \delta\eta$ to leading order, where $\delta\eta$ is a infinitesimal increment. Hence,

$$\mathcal{T}'(z) = \frac{\delta(\hat{\eta}^2)}{\delta(\eta^2)} = \frac{\hat{\mathcal{A}}}{\mathcal{A}} \left(e^{2\pi/C} + O(\sqrt{\varepsilon}) \right).$$

To compute the integral in (5.4) consider U a neighbourhood of the saddle where it can be \mathcal{C}^1 -linearised by Hartman's theorem in 2 dimensions. We can choose U independent of ε and such that γ intersects the boundary transversely for η close to η_0 . Then, the time spent outside U is bounded so the contribution of the integral there is $O(\sqrt{\varepsilon})$. The contribution in U can be computed after linearisation and we get,

$$\int_{\gamma} \tau dt = T\tau_{\text{sad}} + O(\sqrt{\varepsilon}) = T(\tau_0 + O(\varepsilon)) + O(\sqrt{\varepsilon}),$$

where T is the time spent at U and in the second equality we approximate to first order τ at the saddle by evaluating (5.3) at $x_g + \frac{1}{2}$ so,

$$\tau_0 = -2\pi\sqrt{\varepsilon}(2\sin 2\pi x_g + \tilde{\alpha}).$$

The time T can also be computed after the linearisation. If we let λ be the unstable eigenvalue we find,

$$T = \frac{-1}{\lambda} \log \frac{\eta - \eta_s}{k_1} = \frac{-1}{\lambda} \log \frac{z - z_s}{k + O(\sqrt{\varepsilon})}$$

where k_1 is around⁴ 1, $k = 2\eta_s k_1$ is also around 1 as $\eta_s \sim \sqrt{-\rho_0}/\pi$ and in the second equality we use that η is close to η_s . Consequently,

$$\mathcal{T}'(z) = \left(e^{2\pi/C} + O(\sqrt{\varepsilon}) \right) \left(\frac{z - z_s}{k + O(\sqrt{\varepsilon})} \right)^{\nu\sqrt{\varepsilon} + O(\varepsilon)}, \quad (5.5)$$

where $\nu = -\frac{\tau_0}{\sqrt{\varepsilon}\lambda} > 0$ and is around 1 as we are to the right of the trace-zero curve and outside a neighborhood of the K point. We are interested in points with slope 1 or equivalently,

$$z - z_s = (k + O(\sqrt{\varepsilon})) \left(e^{-2\pi/C} + O(\sqrt{\varepsilon}) \right)^{\frac{1}{\nu\sqrt{\varepsilon} + O(\varepsilon)}}. \quad (5.6)$$

We can compute the transit map by integrating \mathcal{T}' while using that $T(z_s) = z_u$, so

$$\mathcal{T}(z) = z_u + \left(k e^{2\pi/C} + O(\sqrt{\varepsilon}) \right) \left(\frac{z - z_s}{k + O(\sqrt{\varepsilon})} \right)^{1 + O(\sqrt{\varepsilon})}. \quad (5.7)$$

We note that some error terms of \mathcal{T}' depend on η , so when we integrate treating them as constants we loose some control. In particular, one can check that all the errors in this section before (5.7) have derivatives respect parameters of the same

⁴That is, $k_1 = O(1)$ and $1 = O(k_1)$.

order, whereas we cannot guarantee this for the terms in (5.7) which will be relevant latter.

Recall now that snp correspond to fixed points of \mathcal{T} with slope 1, which by doing some algebra with (5.6) and (5.7) are found when,

$$z_u - z_s = O(1) \left(e^{-2\pi/C} + O(\sqrt{\varepsilon}) \right)^{\frac{1+O(\sqrt{\varepsilon})}{\nu\sqrt{\varepsilon}+O(\varepsilon)}}. \quad (5.8)$$

The right hand side of the expression above is exponentially small in $\sqrt{\varepsilon}$, so to all orders this equation is equivalent to (5.2), i.e. the snp⁺ is indistinguishable to rhc⁺.

However, we cannot conclude that the snp⁺ curve is \mathcal{C}^1 -close to rhc⁺ by simply differentiating (5.8) respect parameters, as we do not have control over the derivatives of the error terms. So instead we consider z defined by (5.6). Then we can compute derivative of $\mathcal{T}(z)$ respect parameters by differentiating under the integral sign, for instance for $\tilde{\alpha}$ we have,

$$\frac{d}{d\tilde{\alpha}} T(z) = \frac{d}{d\tilde{\alpha}} z_u + \int_0^{z-z_s} \frac{d}{d\tilde{\alpha}} T'(\Delta z + z_0) d\Delta z + \frac{d}{d\tilde{\alpha}} (z - z_s).$$

The third term is given by the derivative of the right hand side of (5.6), where the error terms are well behaved, and it is easy to check that this term is exponentially small. For the second term we can differentiate (5.5) respect $\tilde{\alpha}$ as the error terms preserve their order, so we find,

$$\int_0^{z-z_s} \frac{d}{d\tilde{\alpha}} T'(\Delta z + z_0) d\Delta z = O(1/\sqrt{\varepsilon}) \left(e^{-2\pi/C} + O(\sqrt{\varepsilon}) \right)^{\frac{1+O(\sqrt{\varepsilon})}{\nu\sqrt{\varepsilon}+O(\varepsilon)}}.$$

Thus, differentiating $\mathcal{T}(z) = z$ we get

$$\frac{d}{d\tilde{\alpha}} (z_u - z_s) = O(1/\sqrt{\varepsilon}) \left(e^{-2\pi/C} + O(\sqrt{\varepsilon}) \right)^{\frac{1+O(\sqrt{\varepsilon})}{\nu\sqrt{\varepsilon}+O(\varepsilon)}},$$

which is again exponentially small in $\sqrt{\varepsilon}$, so to all orders it is equivalent to the derivative of (5.2). Thus, snp⁺ is \mathcal{C}^1 -close to rhc⁺ in the region parametrised by $\tilde{\alpha}, \tilde{\rho}$.

We can conclude that assumption 9 is satisfied.

ACKNOWLEDGMENTS

We would like to thank David Marín for helpful discussions both in person and through correspondence.

APPENDIX A. GENERIC SADDLE-NODE CURVES

Following [Kuz04], we can first verify the transversality by checking that differential of the map $(\mathbf{x}, \boldsymbol{\Omega}) \mapsto (\mathbf{G}, \det)$ (where \mathbf{G} denotes the vector field) has full rank. As $D_{\boldsymbol{\Omega}} G$ is the identity and $D_{\boldsymbol{\Omega}} \det = \mathbf{0}$, it is enough to check that $D_{\mathbf{x}} \det \neq 0$ at the saddle-nodes. One can easily check that $D_{\mathbf{x}} \det$ and \det do not vanish simultaneously, so the rank condition is satisfied.

The non-degeneracy of the required second-order Taylor coefficient, can be checked following [GH83, Theorem 3.4.1], by

$$\mathbf{p} D_{\mathbf{x}}^2 G_{\mathbf{x}}(\mathbf{q}, \mathbf{q}) \neq 0,$$

where \mathbf{q} and \mathbf{p} are respectively the right and left eigenvectors of eigenvalue zero of $D_{\mathbf{x}} G_{\mathbf{x}}$, the derivative of the vector field respect the first coordinates at \mathbf{x} .

In our case the differential of the vector field is given by (2.5), and using that in a saddle-node $\det = 0$ we find,

$$\mathbf{p} = (\cos 2\pi x \quad \sin 2\pi x), \quad \mathbf{q} = (d \quad -\varepsilon)^T,$$

with $d = \frac{\cos 2\pi y}{\cos 2\pi x} = \frac{\sin 2\pi(y-\phi)}{\sin 2\pi x}$, where the equality follows from $\det = 0$ and is always well defined as both denominators do not vanish simultaneously.

We have

$$D_{\mathbf{x}}^2 G_{\mathbf{x}}(\tilde{\mathbf{x}}, \hat{\mathbf{x}}) = 4\pi^2 \begin{pmatrix} \varepsilon \cos 2\pi x \tilde{x}\hat{x} + \sin 2\pi(y-\phi) \tilde{y}\hat{y} \\ \varepsilon \sin 2\pi x \tilde{x}\hat{x} + \cos 2\pi y \tilde{y}\hat{y} \end{pmatrix},$$

so

$$\mathbf{p} D_{\mathbf{x}}^2 G_{\mathbf{x}}(\mathbf{q}, \mathbf{q}) = 4\pi^2 \varepsilon (d^2 + \varepsilon (\cos 2\pi x \cos 2\pi(y-\phi) + \sin 2\pi x \sin 2\pi y)). \quad (\text{A.1})$$

Note that d can not be close to zero, as $\cos 2\pi y$ and $\sin 2\pi(y-\phi)$ do not vanish simultaneously. Thus, (A.1) does not vanish and the saddle-node curves are generic.

APPENDIX B. NON-DEGENERACY OF B POINTS

First, we need to find the B points to first order. As they are in the trace-zero loops, they have $y \sim \pm \frac{1}{4}$ and then substituting y in $\det = 0$ we find $x \sim \pm \frac{1}{4}$ (not necessarily with the same signs).

Without loss of generality we consider the B point on the outer saddle-node curve and near the top of the resonance region, i.e. $x, y \sim \frac{1}{4}$. Similarly to the previous section, checking that the rank of the differential of the map $(\mathbf{x}, \boldsymbol{\Omega}) \mapsto (\mathbf{G}, \det, \text{tr})$ is maximal, see [Kuz04], is equivalent to the independence of the vectors,

$$D_{\mathbf{x}} \det \sim 4\pi^2 \varepsilon (-C, 1), \quad D_{\mathbf{x}} \text{tr} = 4\pi^2 (O(\varepsilon^2), 1 + O(\varepsilon)),$$

which have been evaluated at the B point. They are clearly independent for ε small enough.

Now the required condition on the second-order Taylor coefficients, is that the terms a, b presented in [BM18] do not vanish. Letting $s = \sin 2\pi x$ and $d = \frac{\sin 2\pi(y-\phi)}{\sin 2\pi x}$ and following the notation in [BM18] we have,

$$A = 2\pi s \begin{pmatrix} \varepsilon & d \\ -\varepsilon^2 d^{-1} & -\varepsilon \end{pmatrix}, \quad B(\tilde{\mathbf{x}}, \hat{\mathbf{x}}) = 4\pi^2 \begin{pmatrix} sd\varepsilon^2 \tilde{x}\hat{x} + \cos 2\pi(y-\phi) \tilde{y}\hat{y} \\ s\varepsilon \tilde{x}\hat{x} + \sin 2\pi y \tilde{y}\hat{y} \end{pmatrix}$$

so,

$$\mathbf{q}_0 = \begin{pmatrix} d \\ -\varepsilon \end{pmatrix}, \quad \mathbf{q}_1 = \frac{d}{2\pi s(d^2 + \varepsilon^2)} \begin{pmatrix} \varepsilon \\ d \end{pmatrix}$$

and,

$$\mathbf{p}_0 = \frac{1}{d^2 + \varepsilon^2} (d \quad -\varepsilon), \quad \mathbf{p}_1 = 2\pi s (\varepsilon d^{-1} \quad 1).$$

Now, using that $s \sim 1$ and $d \sim C$ we can compute,

$$\begin{aligned} a &= \frac{1}{2} \mathbf{p}_1 B(\mathbf{q}_0, \mathbf{q}_0) = 2\pi^2 C^2 \varepsilon + O(\varepsilon^2), \\ b &= \mathbf{p}_0 B(\mathbf{q}_0, \mathbf{q}_0) + \mathbf{p}_1 B(\mathbf{q}_0, \mathbf{q}_1) = -4\pi^2 \varepsilon + O(\varepsilon^2). \end{aligned}$$

Thus, for ε small enough, the coefficients are non-zero and we can conclude that the B point is generic.

APPENDIX C. LYAPUNOV COEFFICIENT OF THE CENTRES

As for the other bifurcations we check the transversality condition by noting that in the top/bottom of the resonance region,

$$D_{\mathbf{x}} \text{tr} = 4\pi^2(O(\varepsilon), \pm 1 + O(\varepsilon)) \neq 0,$$

so the differential of the map $(\mathbf{x}, \boldsymbol{\Omega}) \mapsto (\mathbf{G}, \text{tr})$ has maximal rank.

We now want to find the Lyapunov coefficient of the centres on the trace-zero curves to check that we have a non-degenerate Hopf bifurcation.

We follow [Kuz04] by first finding an affine coordinate change,

$$\tilde{\mathbf{x}} = \begin{pmatrix} a & b \\ c & d \end{pmatrix} \delta \mathbf{x}, \quad (\text{C.1})$$

where $\delta \mathbf{x} = \mathbf{x} - \mathbf{x}_0$, with $\Delta = ad - bc \neq 0$ and inverse

$$\delta \mathbf{x} = \frac{1}{\Delta} \begin{pmatrix} d & -b \\ -c & a \end{pmatrix} \tilde{\mathbf{x}},$$

to reduce the linearised dynamics around the centre \mathbf{x}_0 to the form,

$$\dot{\tilde{\mathbf{x}}} = \begin{pmatrix} 0 & -\omega \\ \omega & 0 \end{pmatrix} \tilde{\mathbf{x}}. \quad (\text{C.2})$$

The equilibria with $\text{tr} = 0$ can be parametrised by $x_0 \in \mathbb{R}$ and the choice of root y_0 of $\cos 2\pi y_0 = \varepsilon \sin 2\pi x_0$ close to $\frac{1}{4}$ (resp. $-\frac{1}{4}$) for the top (resp. bottom) of the resonance region. For the moment we restrict our attention to the top of the resonance region. On $\text{tr} = 0$, the linearisation of the vector field in $\delta \mathbf{x}$ -coordinates (2.5) has the form,

$$\dot{\delta \mathbf{x}} = 2\pi \begin{pmatrix} \varepsilon S_0 & C\Gamma - \varepsilon S S_0 \\ -\varepsilon C_0 & -\varepsilon S_0 \end{pmatrix} \delta \mathbf{x},$$

where $S_0 = \sin 2\pi x_0$, $C_0 = \cos 2\pi x_0$ and $\Gamma = \sqrt{1 - \varepsilon^2 S_0^2}$ (the positive root corresponds to the centres at the top of the resonance region). On centres the determinant is positive so

$$4\pi^2 \varepsilon (CC_0\Gamma - \varepsilon S_0(SC_0 + S_0)) > 0.$$

In particular, for ε small enough we have $C_0 > 0$. Moreover, as the determinant is invariant under change of bases, we have

$$\omega^2 = 4\pi^2 \varepsilon (CC_0\Gamma - \varepsilon S_0(SC_0 + S_0)),$$

and to simplify notation we write

$$\omega = 2\pi f_0, \quad f_0 = \sqrt{\varepsilon (CC_0\Gamma - \varepsilon S_0(SC_0 + S_0))}.$$

The equations for the coordinate change (C.1) are given by,

$$2\pi \begin{pmatrix} \varepsilon S_0 a - \varepsilon C_0 b & (C\Gamma - \varepsilon S S_0)a - \varepsilon S_0 b \\ \varepsilon S_0 c - \varepsilon C_0 d & (C\Gamma - \varepsilon S S_0)c - \varepsilon S_0 d \end{pmatrix} = 2\pi \begin{pmatrix} -f_0 c & -f_0 d \\ f_0 a & f_0 b \end{pmatrix}.$$

As the equations are linearly dependent we have two degrees of freedom (scaling and rotation) in the choice of solution. We have chosen

$$a = f_0, \quad b = f_0, \quad c = \varepsilon(C_0 - S_0), \quad d = -C\Gamma + \varepsilon S_0(S + 1).$$

The determinant of this change of variable is given by,

$$\Delta = -f_0(C\Gamma + \varepsilon C_0 - \varepsilon S_0(S + 2)) =: -f_0 \Delta_0.$$

Taylor expanding the vector field (#) about the centre \mathbf{x}_0 to third order in $\delta\mathbf{x}$ yields,

$$\begin{aligned}\dot{\delta x} &= 2\pi(\varepsilon S_0 \delta x + (C\Gamma - \varepsilon S S_0)\delta y) + 2\pi^2(\varepsilon C_0 \delta x^2 + (S\Gamma + \varepsilon C S_0)\delta y^2) \\ &\quad - \frac{4}{3}\pi^3(\varepsilon S_0 \delta x^3 + (C\Gamma - \varepsilon S S_0)\delta y^3) \\ \dot{\delta y} &= -2\pi(\varepsilon C_0 \delta x + \varepsilon S_0 \delta y) + 2\pi^2(\varepsilon S_0 \delta x^2 + \Gamma \delta y^2) + \frac{4}{3}\pi^3(\varepsilon C_0 \delta x^3 + \varepsilon S_0 \delta y^3).\end{aligned}$$

We have already designed the change of variables to put the linear part in the form of (C.2), so we write the transformed vector field to third order as

$$\dot{\tilde{\mathbf{x}}} = \begin{pmatrix} 0 & -\omega \\ \omega & 0 \end{pmatrix} \tilde{\mathbf{x}} + \begin{pmatrix} P \\ Q \end{pmatrix}.$$

We compute,

$$\begin{aligned}P &= \frac{2\pi^2}{\Delta^2} \left((a\varepsilon C_0 + b\varepsilon S_0)(d\tilde{x} - b\tilde{y})^2 + (a(S\Gamma + \varepsilon C S_0) + b\Gamma)(-c\tilde{x} + a\tilde{y})^2 \right) \\ &\quad + \frac{4\pi^3}{3\Delta^3} \left((-a\varepsilon S_0 + b\varepsilon C_0)(d\tilde{x} - b\tilde{y})^3 + (-a(C\Gamma - \varepsilon S S_0) + b\varepsilon S_0)(-c\tilde{x} + a\tilde{y})^3 \right)\end{aligned}$$

and,

$$\begin{aligned}Q &= \frac{2\pi^2}{\Delta^2} \left((c\varepsilon C_0 + d\varepsilon S_0)(d\tilde{x} - b\tilde{y})^2 + (c(S\Gamma + \varepsilon C S_0) + d\Gamma)(-c\tilde{x} + a\tilde{y})^2 \right) \\ &\quad + \frac{4\pi^3}{3\Delta^3} \left((-c\varepsilon S_0 + d\varepsilon C_0)(d\tilde{x} - b\tilde{y})^3 + (-c(C\Gamma - \varepsilon S S_0) + d\varepsilon S_0)(-c\tilde{x} + a\tilde{y})^3 \right)\end{aligned}$$

The first Lyapunov coefficient, see [Kuz04], is

$$\begin{aligned}l_1 &= \frac{1}{8\omega} (P_{xxx} + P_{xyy} + Q_{xxy} + Q_{yyy}) \\ &\quad + \frac{1}{8\omega^2} (P_{xy}(P_{xx} + P_{yy}) - Q_{xy}(Q_{xx} + Q_{yy}) - P_{xx}Q_{xx} + P_{yy}Q_{yy}),\end{aligned}$$

where we have dropped the tildes from x and y and the derivatives are evaluated at 0. We will only need to compute this coefficient to first order on ε , so we use the following approximations,

$$\begin{aligned}\Gamma &\sim 1, & f_0 &\sim \sqrt{\varepsilon C C_0}, & \Delta_0 &\sim C, \\ a &\sim \sqrt{\varepsilon C C_0}, & b &\sim \sqrt{\varepsilon C C_0}, & c &= \varepsilon(C_0 - S_0), & d &\sim -C.\end{aligned}$$

The P terms are

$$\begin{aligned}P_{xx} &\sim \frac{4\pi^2\varepsilon}{f_0}(C_0 + S_0) \\ P_{xy} &\sim \frac{4\pi^2\varepsilon}{C^2}((C - S - 1)C_0 + (C + S + 1)S_0) \\ P_{yy} &\sim \frac{4\pi^2 f_0}{C^2}(S + 1) \\ P_{xxx} &\sim \frac{8\pi^3\varepsilon}{f_0^2}(C_0 - S_0) \\ P_{xyy} &= 0.\end{aligned}$$

The Q terms are

$$\begin{aligned} Q_{xx} &\sim -\frac{4\pi^2\varepsilon}{f_0^2}CS_0 \\ Q_{xy} &\sim \frac{4\pi^2\varepsilon}{Cf_0}(C_0 - (C+1)S_0) \\ Q_{yy} &\sim -\frac{4\pi^2}{C} \\ Q_{yyy} &= o(\varepsilon) \\ Q_{xxy} &\sim -\frac{8\pi^3\varepsilon}{f_0^2}C_0. \end{aligned}$$

Finally we compute,

$$l_1 \sim -\frac{\pi^2\varepsilon}{2CC_0f_0^3}(CS_0^2 + S_0C_0 + SC_0^2), \quad (\text{C.3})$$

and we note that $C_0, f_0 > 0$. So we have that $l_1 < 0$ as long as the bilinear form (on S_0 and C_0) inside the parentheses is positive definite. The condition of positive definiteness reduces to,

$$CS - \frac{1}{4} > 0,$$

or equivalently $\phi \in (\frac{1}{24}, \frac{5}{24})$ (assuming $\phi \in (-\frac{1}{4}, \frac{1}{4})$ which is needed to avoid degenerate cases of the ellipse ψ).

Recall that we have restricted our attention to the top of the resonance region. On the bottom, similar computations also yield (C.3), where in this case $C_0 < 0$ so $l_1 > 0$. Thus, the first Lyapunov coefficient is non-zero and the bifurcation is generic.

APPENDIX D. AVERAGE OF f IN CHC IS BIGGER THAN $f(x_{\text{sad}})$

To show that the average of f over the region bounded by chc (weighted by $e^{2\pi x/C}$) is bigger than $f(x_{\text{sad}})$ it will be convenient to write,

$$f(x) = \sqrt{(C-S)^2 + 1} \cos 2\pi(x - x_f),$$

where $x_f = \frac{\arctan(C-S)}{2\pi}$, again with the standard arctangent determination.

Let us consider first $\rho > \rho_0$, and denote by I_ρ the interval of x where the chc is defined, so that x_{sad} is its right endpoint. One can prove, exactly in the same way as in [BM18], that the minimum of g in the I_ρ is achieved in the saddle⁵. Now as $x_f \leq x_g$ and they represent the phase shift of f and g respectively, the minimum of f in I_ρ is also at x_{sad} , as long as I_ρ does not contain a local minimum of f . Finding when x_{sad} meets the first local minimum $x_f + \frac{1}{2}$, one deduces that for $\rho \in (\rho_t, 1)$, where

$$\rho_t = -\frac{C-S}{\sqrt{2-2CS}},$$

we have $f(x) \geq f(x_{\text{sad}})$ in the chc, and thus the average is also bigger.

Consider now $\rho \in (\rho_0, \rho_t)$. We need to prove that,

$$\int_\gamma (f(x) - f(x_{\text{sad}}))e^{-2\pi x/C} \eta dx > 0. \quad (\text{D.1})$$

⁵For $\phi = 0$, as was the case in [BM18], we are done as $f = g$.

We do this by bounding the positive and negative contributions of the integrand separately. As f is symmetric about the minimum $x_f + \frac{1}{2}$, we have that the integrand is negative exactly in $[x_{\text{mid}}, x_{\text{sad}}]$ where $x_{\text{mid}} = 2x_f + 1 - x_{\text{sad}}$. Denote by η_{max}^- the maximum of η in this interval. For the positive contribution it is convenient to only consider the interval $[x_{\text{cen}}, x_{\text{mid}}]$ and denote by η_{min}^+ for the minimum η in it. So we find that it is enough to show that

$$\eta_{\text{min}}^+ \int_{x_{\text{cen}}}^{x_{\text{mid}}} (f(x) - f(x_{\text{sad}})) e^{-2\pi x/C} dx > \eta_{\text{max}}^- \int_{x_{\text{mid}}}^{x_{\text{sad}}} (f(x_{\text{sad}}) - f(x)) e^{-2\pi x/C} dx,$$

which by integrating is equivalent to,

$$\eta_{\text{min}}^+ F(x_{\text{cen}}) > \eta_{\text{max}}^- F(x_{\text{sad}}) - (\eta_{\text{max}}^- - \eta_{\text{min}}^+) F(x_{\text{mid}}),$$

where

$$F(x) = \frac{C e^{-2\pi x/C}}{2\pi(1+C^2)} \left(f(x) + \frac{C}{2\pi} f'(x) - (1+C^2)f(x_{\text{sad}}) \right).$$

From the symmetry of f about the minimum $x_f + \frac{1}{2}$ we have that $f(x_{\text{mid}}) = f(x_{\text{sad}})$ and $f'(x_{\text{mid}}) = -f'(x_{\text{sad}})$. Using this together with the fact that $\sin 2\pi x_{\text{sad}} = \sin 2\pi x_{\text{cen}} = \rho$ one can show that the term inside the parenthesis of $F(x_{\text{cen}})$ is positive and bigger than the ones inside $F(x_{\text{sad}})$ and $-F(x_{\text{mid}})$. Thus, it is enough to show that,

$$\eta_{\text{min}}^+ e^{-2\pi x_{\text{cen}}/C} > \eta_{\text{max}}^- e^{-2\pi x_{\text{sad}}/C} + (\eta_{\text{max}}^- - \eta_{\text{min}}^+) e^{-2\pi x_{\text{mid}}/C}. \quad (\text{D.2})$$

Now looking at the nullclines of the Hamiltonian system (3.1), we find that $\eta(x)$ has a unique relative extremum \tilde{x} , which is a maximum with value $\sqrt{\sin 2\pi \tilde{x} - \rho} / (\pi \sqrt{2})$. Thus, η_{max}^- is bounded by π^{-1} , and η_{min}^+ is attained either at x_{cen} or at x_{mid} . In the latter case, we have $\eta_{\text{max}}^- = \eta_{\text{min}}^+$, so (D.2) becomes, $e^{-2\pi(x_{\text{cen}} - x_{\text{sad}})/C} > 1$ which is satisfied as $x_{\text{cen}} < x_{\text{sad}}$.

If η_{min}^+ is attained at x_{cen} , we have,

$$(\eta_{\text{min}}^+)^2 = \frac{C}{2\pi^2(1+C^2)} \left(\sqrt{1-\rho^2} - C\rho + e^{-2\pi(x_{\text{sad}} - x_{\text{cen}})/C} (\sqrt{1-\rho^2} + C\rho) \right).$$

We note that the second term inside the parenthesis is positive since $\rho > \rho_0$, so we can bound the exponential by $e^{-2\pi/C}$ and η_{min}^+ is bounded below by $l(\rho)$ where,

$$l(\rho) = \frac{\sqrt{C}}{\sqrt{2\pi}\sqrt{1+C^2}} \sqrt{(1+e^{-2\pi/C})\sqrt{1-\rho^2} - (1-e^{-2\pi/C})C\rho}.$$

Note that l is concave so that $\eta_{\text{min}}^+ \geq \min(l(\rho_0), l(\rho_t))$. For $\rho > \rho_0$ we also have $x_{\text{sad}} = \frac{1}{2} - x_{\text{cen}}$, so that $x_{\text{cen}} - x_{\text{mid}} = 2x_f - \frac{1}{2}$. Then, if in (D.2) we bound the difference of η 's by η_{max}^- which in turn we bound by π^{-1} and we also bound the exponentials of the right hand side by $e^{-2\pi x_{\text{mid}}/C}$, we find that it is enough to show,

$$e^{-2\pi(2x_f - \frac{1}{2})/C} > \frac{2}{\pi \min(l(\rho_0), l(\rho_t))}.$$

It is not hard to check that this inequality is true for $\phi \in (\frac{1}{24}, \frac{5}{24})$.

Similar arguments can be done for $\rho < \rho_0$.

REFERENCES

- [BLM22] C. N. Baesens, F. Di Lallo, and R. S. MacKay. Corrigendum: simplest bifurcation diagrams for monotone families of vector fields on a torus (2018 nonlinearity 31 2928). *Nonlinearity*, 35(5):C5–C8, 2022. DOI: 10.1088/1361-6544/ac5de3.
- [BM18] C. Baesens and R. S. MacKay. Simplest bifurcation diagrams for monotone families of vector fields on a torus. *Nonlinearity*, 31(6):2928–2981, 2018. DOI: 10.1088/1361-6544/aab6e2.
- [GH83] John Guckenheimer and Philip Holmes. *Nonlinear Oscillations, Dynamical Systems, and Bifurcations of Vector Fields*. Springer, New York, 1st edition, 1983.
- [Kuz04] Yuri Kuznetsov. *Elements of Applied Bifurcation Theory*. Springer-Verlag, New York, 3rd edition, 2004.
- [Per94] L. M. Perko. Homoclinic loop and multiple limit cycle bifurcation surfaces. *Transactions of the American Mathematical Society*, 344(1):101–130, 1994.